in which case $U_{\text{eff}}\eta_0=1.7$. The Stoner condition is

$$-U_{\text{eff}}(P,T_c)\int_{-\infty}^{\infty}\frac{\partial}{\partial\epsilon}f(\epsilon)\eta(\epsilon)d\epsilon=1$$

at $T=T_c=631°\text{K}$. This would seem to imply $U_{\text{eff}}(P,0)\times\eta_0\approx 1$, in contradiction to $\frac{1}{3}U\eta_0=1.7$. If U_{eff} is magnetization-dependent, this discrepancy will not arise. This gives some indication that U is in fact large. The most important point is that the magnetization dependence of U_{eff} can lead to an estimate of U.

We wish to thank Dr. Hubbard for bringing to our attention the term in (4) that was neglected by Kanamori and for a number of other helpful comments.

PHYSICAL REVIEW VOLUME 177, NUMBER 2 10 JANUARY 1969

Critical Scattering of Sound in Rare-Earth Metals*

R. J. Pollina and B. Lüthi
Department of Physics, Rutgers, The State University, New Brunswick, New Jersey 08903
(Received 8 July 1968)

We present ultrasonic attenuation measurements in the vicinity of the Néel temperature for terbium, dysprosium, and holmium. Longitudinal sound waves along the c axis exhibit a large critical attenuation, whereas shear waves show only a small but measurable effect in dysprosium. The spin-phonon coupling responsible for this critical attenuation is predominantly of volume-magnetostrictive character for longitudinal waves and of linear-magnetostrictive (single-ion-type) character for shear waves. Longitudinal wave attenuation in the paramagnetic region gives the following critical exponent η [$\alpha\propto\omega^2(T-T_N)^{-\eta}$]: terbium 1.24 ± 0.1, dysprosium 1.37 ± 0.1, holmium 1.0 ± 0.1. Shear waves in dysprosium give $\eta=0.8\pm0.15$. These exponents, with the exception of the shear-wave case, can be fairly well accounted for by recent theories of ultrasonic attenation at magnetic phase transitions. The critical exponent η for shear waves in Dy, together with the magnitude of the effect, can tentatively be explained with present theories by considering higher-order terms in the spin-phonon coupling. For temperatures very close to T_N the attenuation remains finite. We show this to be an impurity effect.

I. INTRODUCTION

We present results of a systematic study of the critical scattering of ultrasound in the paramagnetic region of the heavy rare-earth metals terbium (Tb), dysprosium (Dy),[1] and holmium (Ho). Similar experimental results for gadolinium (Gd) were reported earlier.[2] There is a noticeable lack of experimental information on the behavior of transport coefficients at phase transitions. One can gain such information, for example, by studying the ultrasonic attenuation at magnetic phase transitions. On the one hand, the rare-earth metal series is an attractive subject for such a study because the magnetic and elastic properties vary in a rather systematic way and because the magnetoelastic properties have been studied extensively in recent years. On the other hand, impurities are a serious problem in these metals. We shall show how they influence the ultrasonic attenuation and how this effect can be separated from the critical scattering of sound. Since the nature of the interaction seems to be very important in determining the critical behavior,[3] we shall also put emphasis on the discussion of the coupling mechanism as before.[2] Our result of this investigation will show that the critical scattering of sound is indeed very sensitive to the nature of the coupling mechanism and in this way to the form of the spin-correlation function.

In Sec. II we discuss experimental details. Then we present experimental results which enable us to determine the spin-phonon coupling mechanism which is responsible for critical scattering. Finally, we give quantitative results for the paramagnetic region and discuss these in the light of recent theories.

II. EXPERIMENT

We investigated two single crystals of Dy (DyA and DyB) and one single crystal each of Tb and Ho. DyA and Ho were grown by R. J. Gambino of the IBM Watson Research Center, whereas Tb and DyB were purchased from Metals Research Ltd. The crystals were spark-cut into cylindrical form, carefully oriented along the c axis, and finally ground and polished to parallelicity within optical accuracy. X-ray pictures revealed clear spots, indicating good quality crystals.

In Table I we have listed some properties of these crystals: Columns 2 and 3 give the longitudinal and shear velocities measured for our crystals for sound wave propagation along the c direction. Column 1 shows the ultrasonically determined Néel temperatures T_N of

* Work supported by the National Science Foundation and the Rutgers Research Council.
[1] R. J. Pollina and B. Lüthi, Bull. Am. Phys. Soc. 13, 616 (1968).
[2] B. Lüthi and R. J. Pollina, Phys. Rev. 167, 488 (1968).
[3] L. P. Kadanoff, Comments Solid State Phys. 1, 5 (1968).

TABLE I. Néel temperatures, longitudinal and transverse sound velocities for our rare-earth crystals.

	T_N (°K)	V_l (10^5 cm/sec)	V_t (10^5 cm/sec)
Gd	290.4	3.20	1.64
Tb	227.6	3.10	1.66
Dy	177.3	3.10	1.74
Ho	132.1	3.22	1.76

these crystals. With the exception of Ho, these crystals all exhibit somewhat smaller T_N than for the purest samples reported in the literature. The critical scattering of sound, discussed below, shows similarly the smallest impurity effect for Ho.

The attenuation was measured using longitudinal and shear waves in the frequency range 30–170 Mc/sec and using standard ultrasonic pulse-echo techniques. Whereas the longitudinal wave pattern could easily be tuned into an exponential form, we encountered some difficulties with the shear-wave pattern in Dy. However, since the form of the pattern stayed approximately constant over the small temperature range covered, we could take any echo difference for this relative measurement. The longitudinal attenuation in the critical region is rather large, whereas the shear-wave attenuation is small. But even in the shear-wave case (Dy), estimated diffraction losses are negligible and contribute only to the background attenuation.

Special care was taken for the temperature measurement and control. The samples were mounted in a solid piece of brass and the sample holder surrounded by a 1-cm-thick brass cylinder. The temperature and the temperature gradients were measured with copper-constantan or gold-cobalt thermocouples. In addition to a heater with feedback control, the temperature was stabilized by a liquid-nitrogen–ethanol bath for Tb and Dy and a liquid-nitrogen bath for Ho. A typical temperature stability was better than 0.01°C and the temperature gradient across the sample was approximately 0.01°C.

III. COUPLING MECHANISM

We first show some experimental results which enable us to determine the spin-phonon coupling mechanism. Figures 1–3 show experimental results of attenuation of 50-Mc/sec compressional and shear waves for Tb, Dy, and Ho, respectively, in the neighborhood of the Néel temperature T_N. At T_N these metals show a transition from paramagnetic to a spiral arrangement of the spins.

As seen from these figures, for all three metals there is a pronounced increase in attenuation for longitudinal waves in the paramagnetic region as T_N is approached. With the exception of Tb there is a sharp peak at T_N with a subsequent decrease in attenuation in the ordered region. For Tb it is probably the vicinity of the ferromagnetic Curie point T_c which forces the attenuation to show only a shoulder at T_N instead of a peak and to

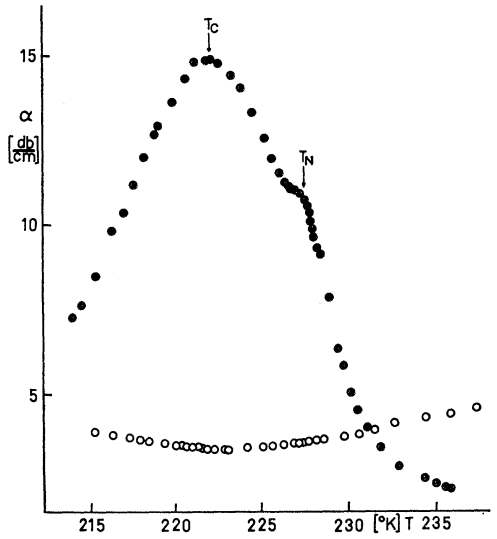

FIG. 1. Critical attenuation of sound in Tb. Propagation along c axis, $\nu = 50$ Mc/sec. ●, longitudinal; ○, transverse.

rise somewhat more slowly until T_c. The behavior of Dy and Ho is very similar to the one observed in Gd.[2]

For shear waves, on the other hand, we do not observe any noticeable anomaly at T_N for Tb and Ho, but a well-established peak in Dy. As mentioned above, great care was taken to orient the crystals carefully. Therefore, in contrast to the case of Gd, the shear-wave peak in Dy cannot be produced by shear waves propagating slightly off the c axis. From the c-axis misalignment of less than 0.5° we estimate from the 10-dB/cm longitudinal attenuation peak an induced shear-wave attenuation peak of less than 0.05 dB/cm, whereas the observed one is 0.5 dB/cm. From the misalignment of 2° in c-cut Gd

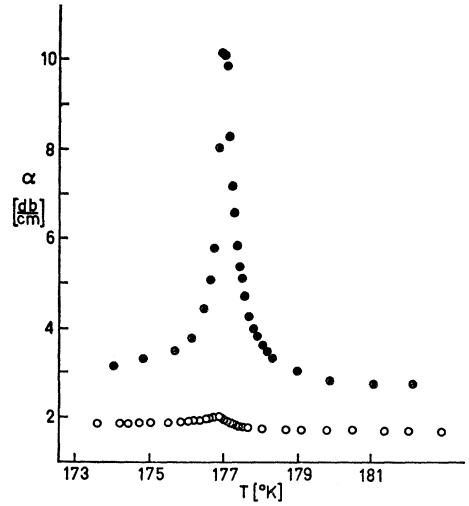

FIG. 2. Critical attenuation of sound in Dy. Propagation along c axis, $\nu = 50$ Mc/sec. ●, longitudinal—DyB; ○, transverse—DyA.

[4] E. Callen and H. B. Callen, Phys. Rev. **139**, 455 (1965).

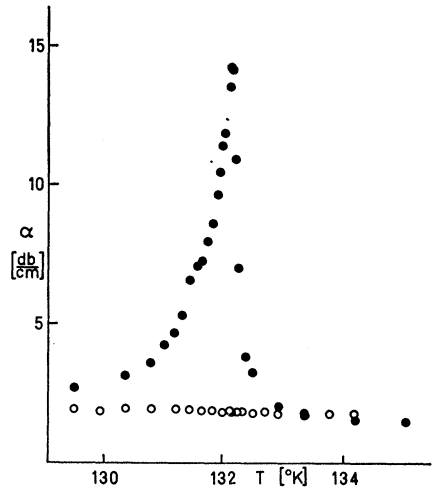

FIG. 3. Critical attenuation of sound in Ho. Propagation along c axis, $\nu=50$ Mc/sec. ●, longitudinal; ○, transverse.

we estimated a 0.5-dB/cm induced shear-wave peak, just the order of the observed one. In the case of Tb we could observe at higher frequencies (150 Mc/sec) that a shear-wave peak also developed. However, the rather high background attenuation prevented us from taking quantitative measurements.

The results of Figs. 1–3, together with the corresponding results for Gd,[2] enable us to discuss the coupling-constant mechanism. This we do by relating our results to measured magnetostriction constants. The magnetoelastic Hamiltonian for hexagonal symmetry, linear in the strain components and quadratic in the spin operators, follows[4]: (a) for longitudinal sound propagating in the c direction,

$$\mathcal{H}_{me}=\epsilon_{zz}\{\sum_i B_i[(S_i^z)^2-\tfrac{1}{3}S(S+1)]+\sum_{ij} D_{ij}\mathbf{S}_i\cdot\mathbf{S}_j+\sum_{ij} D_{ij}'(S_i^zS_j^z-\tfrac{1}{3}\mathbf{S}_i\cdot\mathbf{S}_j)\}; \quad (1a)$$

(b) for shear waves propagating in the c direction,

$$\mathcal{H}_{me}=\epsilon_{xz}\{\sum_i b_i(S_i^xS_i^z+S_i^zS_i^x)+\sum_{ij} d_{ij}(S_i^xS_j^z+S_i^zS_j^x)\}, \quad (1b)$$

with a similar term involving the (y,z) components. Here B_i, b_i and D_{ij}, D_{ij}', d_{ij} are, respectively, the so-called single-ion and two-ion magnetoelastic coupling constants which are temperature-independent. They are related to the temperature-dependent magnetostriction constants through the various spin-correlation functions.[4]

Magnetostriction experiments show[5,6] that in Gd the d and b constants are of the same order, but that b in Dy is much larger than d. In column 2 of Table II we have listed the constants b for our metals. We estimated them from the approximate relation for the magnetostriction constants[6] $\lambda^{\epsilon,2}/\lambda^{\gamma,2}\simeq 0.6$, taking the $\lambda^{\gamma,2}$ constants at $T=0$ from the literature[5–8] and relating $\lambda^{\epsilon,2}$ to b by $b=4c_{44}\lambda^{\epsilon,2}$ (c_{44} values are calculated from the shear-wave velocities listed in Table I). In the case of Tb the estimated value agrees roughly with values determined experimentally from linear magnetoelastic birefringence experiments[9] and also with values from the magnetoelastic splitting of the spin-wave dispersion spectrum as measured by inelastic neutron scattering.[10]

TABLE II. Comparison of magnetoelastic coupling constants with critical sound attenuation: Coupling constants have been normalized to reduced magnetization.

	Volume magnetoelastic coupling constant D (10^6 erg/cc)	Linear magnetoelastic coupling constant b (10^6 erg/cc)	Attenuation of 50-Mc/sec sound for $\epsilon=0.01$ (dB/cm) Long.	Shear	Uniaxial anisotropy constants at $T=0$°K (10^6 erg/cc)
Gd	9000	20	1.6	···	3
Tb	7500	1280	3.9	<0.01	550
Dy	3600	1440	0.7	0.05	550
Ho	2200	460	0.5	···	35

The volume magnetostrictive coupling constants $D_{ij}=\partial J_{ij}/\partial\epsilon_{zz}$ were estimated from the pressure dependence[11] of the Néel temperature T_N as explained in a previous paper.[2] They are listed in column 1 of Table II. Since these pressure experiments were performed on polycrystalline materials, these values represent only orders of magnitude and are slightly underestimated.

For the remaining B and D' constants, which arise from the strain modulation of the large uniaxial anisotropy and of the anisotropic exchange, respectively, little quantitative information is known. For Gd both B and D' are of the order of b and therefore rather small, but in Dy and Tb they can be of the order of D. In Ho, on the other hand, they are again smaller.[5–8] They seem to scale roughly to the corresponding single-ion anisotropy constant and to the corresponding anisotropic exchange constant. The $T=0$°K uniaxial anisotropy constants for these metals[12–14] are listed in column 5 of Table II. The value for Ho was calculated from the c-axis magnetization curve.[14]

Columns 3 and 4 of Table II give experimental attenuation results for 50-Mc/sec longitudinal and shear

[5] W. E. Coleman and A. S. Pavlovic, J. Phys. Chem. Solids **26**, 691 (1965).
[6] A. E. Clark, B. DeSavage, and R. M. Bozorth, Phys. Rev. **138**, A216 (1965).
[7] J. J. Rhyne and S. Legvold, Phys. Rev. **138**, A507 (1965).
[8] J. J. Rhyne, S. Legvold, and E. T. Rodine, Phys. Rev. **154**, 266 (1967).
[9] T. Moran and B. Lüthi (to be published).
[10] H. B. Møller, J. C. G. Houmann, and A. R. Mackintosh, J. Appl. Phys. **39**, 807 (1968).
[11] D. B. McWhan and A. L. Stevens, Phys. Rev. **154**, 438 (1967).
[12] J. J. Rhyne and A. E. Clark, J. Appl. Phys. **38**, 1379 (1967).
[13] C. D. Graham, Jr., J. Phys. Soc. Japan **17**, 1310 (1962).
[14] D. L. Standberg, S. Legvold, and F. H. Spedding, Phys. Rev. **127**, 2046 (1962).

waves (background attenuation subtracted) taken at a fixed reduced temperature of $\epsilon=(T-T_N)/T_N=0.01$ in order to compare the different metals.

By comparing the estimated coupling constants (columns 1 and 2) with these attenuation values the following facts are seen.

(a) Whereas, with the exception of Gd, the longitudinal and shear coupling constants (D,b) are of the same order, the experimental shear attenuation values are at least an order of magnitude smaller than the corresponding longitudinal ones.

(b) The variation of the D constant over the four metals corresponds to a similar variation in the longitudinal attenuation values. In fact, the latter varies roughly proportional to D^2. However, no definite statement can be made in view of the approximate estimate of D.

(c) An analogous correspondence of the linear magnetostrictive coupling constant b with the shear-wave attenuation values can also be concluded, although the experimental values are scarce due to the small size of the effect.

(d) The rather large critical attenuation for longitudinal waves in $RbMnF_3$,[15] and especially MnF_2,[16] and the absence of a shear-wave critical attenuation in these substances indicates that the volume magnetostrictive coupling is the dominant mechanism.

From this discussion of the coupling mechanism we can conclude that the order of magnitude of the critical attenuation is dependent in a rather sensitive way on the nature of the coupling mechanism, namely, on the particular spin-correlation function. We can amplify this conclusion somewhat in Sec. IV, where we discuss the quantitative dependence of the ultrasonic attenuation on frequency and temperature.

IV. SOUND ATTENUATION IN PARAMAGNETIC REGION

We focus our attention now on sound-wave attenuation in the paramagnetic region for a quantitative comparison between experiment and theory.

Figures 4–6 show a double logarithmic plot of attenuation (background attenuation subtracted) versus the temperature difference $\Delta T=(T-T_N)$. These are for the case of longitudinal sound waves of various frequencies with propagation along the c axis. The background attenuation was usually taken some 20–30 deg above T_N and assumed to be constant. Measurements of Dy around 230°K and of Ho around 180°K proved this constancy of the background attenuation to be a good assumption. It would affect the anomalous attenuation critically only for frequencies below 30 Mc/sec. For shear waves, because of the small size of the critical attenuation, it can affect the results more seriously.

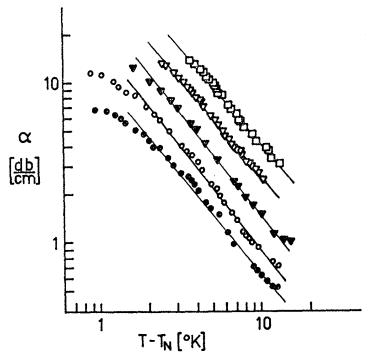

FIG. 4. Temperature dependence of longitudinal ultrasound in Tb. ●, 50 Mc/sec ($\eta=1.22$); ○, 70 Mc/sec ($\eta=1.29$); ▼, 90 Mc/sec ($\eta=1.30$); ▽, 110 Mc/sec ($\eta=1.21$); □, 150 Mc/sec ($\eta=1.19$).

Figures 4–6 show that one has an inverse-power law for the critical attenuation for a region spanning about one decade in ΔT for Tb, almost two decades for Dy, and almost three decades for Ho. The actual power-law region for ϵ is listed in column 3 of Table III. It is seen that the purest sample (Ho) has the widest range for this power law, whereas the least pure sample (Tb) has the narrowest range. The average exponent η for the power-law region $\alpha\propto(T-T_N)^{-\eta}$ is listed in column 1 of Table III for the different materials. The exponent η for the individual frequencies is listed in the captions to Figs. 4–6. The variation of these shows that the individual η varies by not more than ±0.1 for a given material. These η values will be discussed below.

The upper limit of the power-law region ($\Delta T\sim15$–30°K) is determined by the background attenuation. The error in determining the critical attenuation in this region becomes big if this critical attenuation becomes smaller than the background attenuation. The lower

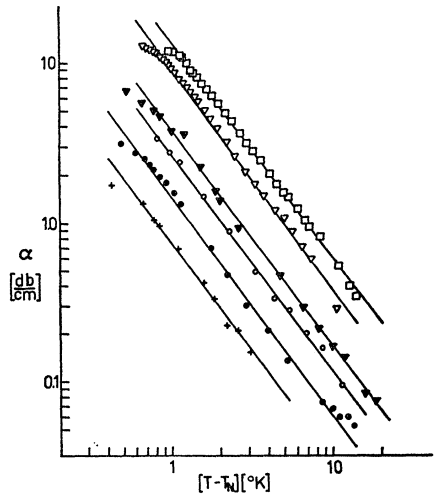

FIG. 5. Temperature dependence of longitudinal ultrasound in dysprosium (DyA). +, 30 Mc/sec ($\eta=1.36$); ●, 50 Mc/sec ($\eta=1.38$); ○, 70 Mc/sec ($\eta=1.36$); ▼, 90 Mc/sec ($\eta=1.37$); ▽, 110 Mc/sec ($\eta=1.39$); □, 150 Mc/sec ($\eta=1.36$).

[15] B. Golding, Phys. Rev. Letters **20**, 5 (1968).
[16] J. R. Neighbours, R. W. Oliver, and C. H. Stillwell, Phys. Rev. Letters **11**, 125 (1963).

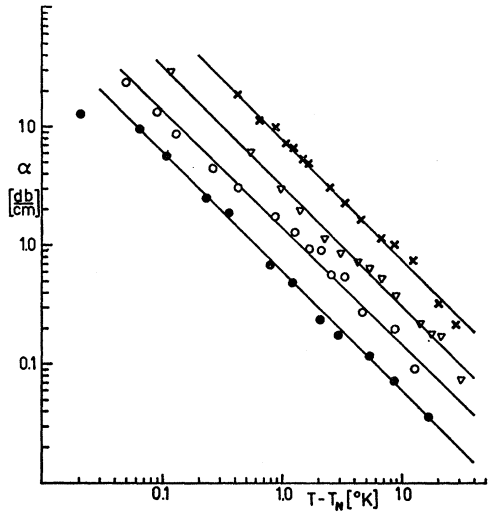

FIG. 6. Temperature dependence of longitudinal ultrasound in Ho. ●, 50 Mc/sec ($\eta=1.01$); ○, 70 Mc/sec ($\eta=0.99$); ▽, 110 Mc/sec ($\eta=1.00$); ×, 170 Mc/sec ($\eta=1.02$).

limit of the power-law region is governed by what we believe is an impurity effect. Figures 4–6 together with Fig. 4 of Ref. 2 show that there is a rolloff of the attenuation for ΔT smaller than 0.8°K for Gd, 1.7°K for Tb, 0.6°K for Dy, and 0.05°K for Ho. For ΔT smaller than these values stated, we were able to fit the attenuation by the following formula: $\alpha \propto \omega^n e^{-\gamma-(T-T_N)^2}$, with $\gamma=2.2K^{-2}$ for Gd, $0.17K^{-2}$ for Tb, $2.1K^{-2}$ for Dy, and $69K^{-2}$ for Ho. The exponent n was usually smaller than 2, about 1.5 for Gd. Figure 7 shows such a fit for Gd, where we have investigated this effect in greatest detail. The Gaussian law above indicates that we have a statistically varying T_N over the sample due to impurities, the half-width of this variation given by $[(\ln 2)/\gamma]^{1/2}$. This impurity controlled attenuation becomes very small for $\Delta T > [\ln(2/\gamma)]^{1/2}$, when the critical attenuation is dominant. It agrees with our earlier conclusion that Ho is the purest, and Tb the least pure sample.

The frequency dependence of the critical attenuation in the temperature region where the power law holds is shown in Figs. 8–10. One can see that an ω^2 law is closely observed, as in the case of Gd. The spin-phonon Hamiltonians (1a), (1b) give an interaction term linear in the strain, and therefore linear in the sound-wave vector q, which leads to a ω^2 dependence for the scattering cross section and the attenuation. As in Gd this is again evidence that one has not to consider coupling

TABLE III. Critical exponents η of sound attenuation $\alpha \propto \omega^2(T-T_N)^{-\eta}$ and power-law range.

	Long.	Trans.	Range of ϵ
Gd(FM)	1.2		10^{-3}–10^{-1}
Tb(AF)	1.24		$7\cdot10^{-3}$–$7\cdot10^{-2}$
Dy(AF)	1.37	0.8±0.15	$3\cdot10^{-3}$–10^{-1}
Ho(AF)	1.0		$3\cdot10^{-4}$–10^{-1}

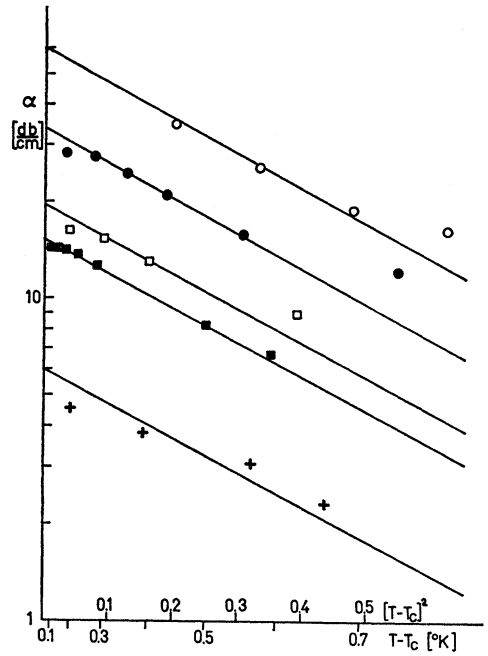

FIG. 7. Critical rolloff of attenuation near T_c in Gd. +, 15 Mc/sec; ■, 30 Mc/sec; □, 36 Mc/sec; ●, 50 Mc/sec; ○, 70 Mc/sec.

mechanisms which are of higher order in the phonon amplitude.

As mentioned above, the only quantitative results for critical attenuation for shear waves we succeeded in getting were in Dy. In Fig. 11 we again show a double logarithmic plot of attenuation versus the temperature difference ΔT. It shows features qualitatively similar to the longitudinal case (Figs. 4–6), namely, a power-law region for about the same temperature interval as in the longitudinal case and a rounding off for smaller ΔT. As already discussed above, the effect is an order of magnitude smaller. The average power-law index η is listed in column 2 of Table III. The error in this index is assumed to be somewhat larger, because of the smallness of the effect and the irregular ultrasonic pattern as

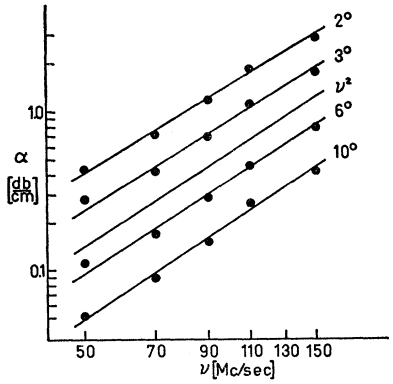

FIG. 8. Frequency dependence of longitudinal ultrasound in Tb. The temperatures of the isotherms are indicated ($\Delta T=2$–10°K).

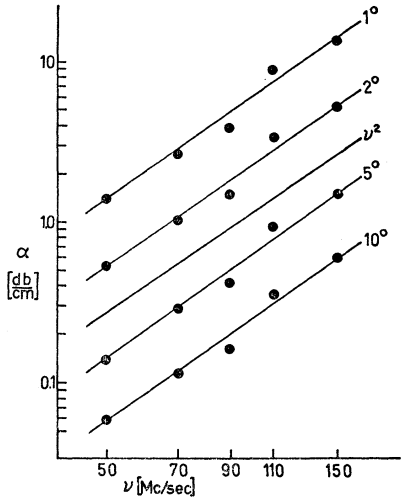

FIG. 9. Frequency dependence of longitudinal ultrasound in Dy. The temperatures of the isotherms are indicated ($\Delta T = 1$–$10°$K).

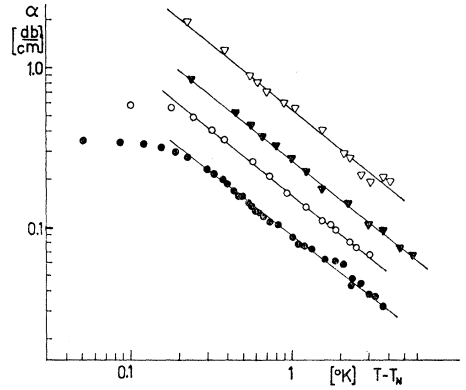

FIG. 11. Temperature dependence of shear ultrasound in dysprosium (DyA). ●, 50 Mc/sec ($\eta = 0.78$); ○, 70 Mc/sec ($\eta = 0.81$); ▼, 90 Mc/sec ($\eta = 0.80$); ▽, 110 Mc/sec ($\eta = 0.82$).

discussed above. We note that this exponent η is quite different from the longitudinal one for Dy.

From the temperature dependence of this shear-wave attenuation for various frequencies shown in Fig. 11, one can also deduce a frequency dependence for a given temperature. The result is again an ω^2 law for the region where the power-law temperature dependence holds. The error is a little larger in this case for the reasons stated.

V. THEORY

As outlined in Ref. 1, using the interaction Hamiltonian (1a) or (1b), one can calculate the ultrasonic attenuation by calculating the rate of destruction of phonons minus the rate of creation of phonons. The result is that the attenuation is proportional to the space-time Fourier transform $G(q,\omega)$ of a four-spin correlation function. This function, in the case where only the volume magnetostrictive coupling D is dominant, is

$$\langle(\mathbf{S}_i\cdot\mathbf{S}_{i+R}(t))(\mathbf{S}_j\cdot\mathbf{S}_{j+R'}(t))\rangle. \tag{2a}$$

Here i, j, R, and R' denote sites and the bracket denotes the average over the equilibrium ensemble. In the case where only the single-ion terms b are important, it is

$$\langle S_i^{\alpha}S_i^{\alpha'}(t)S_j^{\beta}S_j^{\beta'}(t)\rangle, \tag{2b}$$

where i,j again denote sites but α, α', β, and β' label spin components. The crucial point of any theory of ultrasonic attenuation is to calculate $G(q,\omega)$. The two correlation functions (2a) and (2b) have quite different structure and should therefore be able, in principle, to account for the big differences in magnitude and exponent η of longitudinal and shear-wave critical attenuation in Dy.

In the last two years there has been a flurry of theoretical papers dealing with the problem of ultrasonic attenuation at the magnetic phase transition. These theories can be divided roughly into two groups: The first group[17–20] makes two drastic assumptions concerning $G(q,\omega)$. First they start by factorizing the four-spin correlation function into products of two-spin correlation functions. The attenuation coefficient α can then be written as

$$\alpha(q,\omega)=\sum_{k,\omega'}\gamma(k,q)M(k,\omega')M(k-q,\omega'-\omega), \tag{3}$$

where $M(k,\omega)$ is the Fourier transform of the two-spin correlation function and the coupling constant is absorbed with other phonon parameters into $\gamma(k,q)$. Following this they make a second assumption by treating

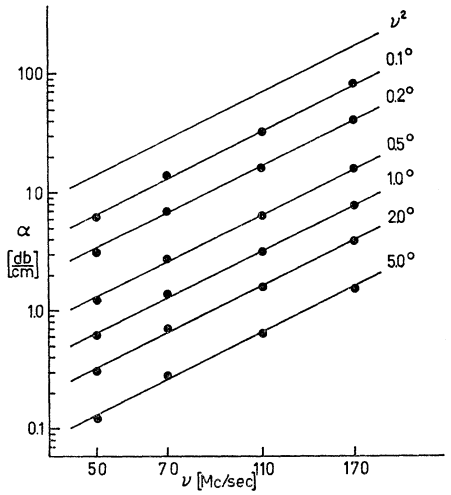

FIG. 10. Frequency dependence of longitudinal ultrasound in Ho. The temperatures of the isotherms are indicated ($\Delta T = 0.1$–$5°$K).

[17] K. Tani and H. Mori, Phys. Letters **19**, 627 (1966); and (to be published).
[18] H. S. Bennett and E. Pytte, Phys. Rev. **155**, 553 (1967); **164**, 712 (1967).
[19] H. Okamoto, Progr. Theoret. Phys. (Kyoto) **37**, 1348 (1967).
[20] K. Kawasaki, Solid State Commun. **6**, 57 (1968).

the $M(k,\omega)$ in the hydrodynamic limit although the sum (k,ω') is not limited to small values. In this manner Bennett and Pytte,[18] for example, can express α in the form $\chi^{3/2}/D$ for ferromagnets and $\chi^{1/2}/D$ for antiferromagnets, where χ is the static susceptibility and D is the spin-diffusion constant. Kawasaki[20] uses scaling-law methods to predict critical exponents. The exponents η derived from these theories are listed in Table IV, where we distinguish between isotropic ferro- and antiferromagnets, as well as between molecular field ferro- and antiferromagnets (see Sec. VI). For example, in the Bennett-Pytte[18] formulas above one takes for the isotropic case $\chi \propto \epsilon^{-4/3}$ and $D \propto \chi^{-1/4}$, whereas in the molecular field case $\chi \propto \epsilon^{-1}$ and $D \propto \chi^{-1}$. It should be noted that these theories give equivalent two-spin correlation functions by factorizing the four-spin functions (2a) and (2b). This is because they start from an isotropic Heisenberg ferromagnet for which it is assumed that $\chi_{ij}=\chi\delta_{ij}$. These theories are therefore not able to explain the difference between our shear-wave and longitudinal results for Dy. A theory for shear-wave attenuation in an anisotropic ferromagnet has not been given so far.[21]

Turning to the second group of ultrasonic attenuation theories, Kawasaki[22] recently proposed a new theory where he circumvents the hydrodynamic approximation in calculating the attenuation coefficient. His theory must therefore be considered the most reliable one for the isotropic case up to date.

VI. COMPARISON OF EXPERIMENT AND THEORY

In another recent paper, Kawasaki[23] gives arguments which show that in cases where one has a strong uniaxial anisotropy or a strong anisotropic exchange, the dynamical behavior of correlation functions is described satisfactorily by the conventional molecular-field theory. On the other hand, for the isotropic-exchange case this conventional treatment breaks down as noted by various groups (see Ref. 23 for references). Therefore we have divided the theoretical results listed in Table IV into two subgroups: isotropic and molecular field.

Referring to our discussion of the spin-phonon coupling constants (see especially column 5 of Table II for values of the uniaxial anisotropy constants), we can approximate Gd and to a lesser extent Ho as isotropic ferro- and antiferromagnets, whereas Tb and Dy are definitely anisotropic antiferromagnets. Therefore, in comparing our experimentally determined η with theory, we relate Gd and Ho to the isotropic case and Tb and Dy to the molecular-field case. We note the following facts: (a) $\eta=1.2$ for Gd is still considerably smaller than the best theoretical value of 1.66; (b) $\eta=1.0$ for Ho is in very good agreement with 1.0 for the isotropic exchange antiferromagnet; (c) $\eta=1.24$ (Tb) and especially $\eta=1.37$ (Dy), representing anisotropic antiferromagnets, lie rather close to the corresponding theoretical value 1.5; (d) the shear-wave exponent for Dy ($\eta=0.8$) is quite different from any theoretical exponent[21]; and (e) in addition, the small exponent $\eta=0.32$ for the isotropic antiferromagnet $RbMnF_3$ is also in bad agreement with theoretical predictions.[15]

TABLE IV. Theoretical critical exponent η for ultrasonic attenuation.

	Ferromagnet		Antiferromagnet	
	Isotropic	Molecular field	Isotropic	Molecular field
Tani and Mori[a]		1		1
Bennett and Pytte[b]	2.3	2.5		1.5
Okamoto[c]		2.5		1.5
Kawasaki[d]	2.2	2.5	1.6	1.5
Kawasaki[e]	1.66		1	

[a] Reference 17.
[b] Reference 18.
[c] Reference 19.
[d] Reference 20.
[e] Reference 22.

In summary, we can conclude the following from our experiments.

(a) The critical attenuation of longitudinal sound in the rare-earth metals occurs predominantly by means of the volume magnetoelastic coupling, whereas the shear-wave critical attenuation arises through the linear magnetoelastic coupling. Although these coupling constants are of the same order of magnitude, at least for Tb and Dy, the shear-wave effect is at least an order of magnitude smaller.

(b) The agreement between experimentally determined critical attenuation exponents η and theoretical values is quite good for the approximately isotropic antiferromagnet Ho, fair for the anisotropic antiferromagnets Tb and Dy, and not so good for the isotropic ferromagnet Gd. The shear-wave critical attenuation exponent can be tentatively explained including higher-order terms in the magnetoelastic interaction.[21]

ACKNOWLEDGMENTS

Further experiments, studying other magnetic substances, are in progress. Discussions with Professor E. Abrahams and Dr. P. Papon are gratefully acknowledged.

[21] Using Kawasaki's method (Ref. 20), appropriate for this case, one can show that terms from Eq. (1b) do not give any singularity. Inclusion of higher-order terms in the magnetoelastic Hamiltonian produces exponents $\eta=\frac{2}{3}$ and $\eta=2.0$, respectively. In this way both the small exponent and the small critical scattering can, in principle, be accounted for. For details, see B. Lüthi, P. Papon, and R. J. Pollina, in Proceedings of the Fourteenth Annual Conference Magnetism and Magnetic Materials, J. Appl. Phys. (to be published).

[22] K. Kawasaki, Phys. Letters **26A**, 543 (1968).

[23] K. Kawasaki, Progr. Theoret. Phys. (Kyoto) **39**, 285 (1968).